

with a quantum-mechanical system and the range of the quantum-mechanical diffraction effects—which is essentially $v_0^{1/3}$ —is as important as the range of the interatomic forces, as at temperatures of the order of the lambda point $v_0^{1/3}$ is about 3.4A. This means that even though we are dealing with a perfect gas, nevertheless there is an interaction sphere around each atom, and its radius is actually larger than that of the classical helium atom. Any influence from the neglected configurations should thus, in our opinion, show up also in the case of the perfect Bose-Einstein gas.

There is another disturbing fact concerning the partition function (F-I.5) or (5). These expressions should be valid for the gas phase of helium, as the approximation (3) should be least inaccurate at high temperatures and low densities. That means that on lowering the

temperature the partition function should reveal the gas-liquid transition before the lambda transition, but this does not happen in the case of (F-I.5) or (5) (compare also the remarks at the end of C-II). This becomes understandable, if we remind ourselves that essentially the attractive forces are neglected in deriving (F-I.5) or (5) (compare the discussion in F-I).

This paper was written while the author was at Purdue University, and I would like to express my thanks to Dr. K. Lark-Horovitz for the hospitality shown to me in his department. In conclusion, I would like to express my gratitude to Dr. R. P. Feynman for pointing out to me some serious mistakes in the first draft of this paper and for making it plausible to me that my original belief that (5) would be exact in the case of hard spheres may not be correct.

Microwave Determination of the Probability of Collision of Electrons in Helium*

LAWRENCE GOULD† AND SANBORN C. BROWN

Department of Physics and Research Laboratory of Electronics, Massachusetts Institute of Technology, Cambridge, Massachusetts

(Received May 10, 1954)

A previously reported microwave method for determining the collision probability for momentum transfer of slow electrons has been modified so that a variation in average electron energy from 0.012 ev to 3 ev may be obtained. Measurements of the ratio of the real part to the imaginary part of the electron conductivity are performed in the afterglow of a pulsed helium discharge in a microwave resonant cavity. The average electron energy is varied by applying a microwave electric field in the afterglow and, under appropriate assumptions, the average electron energy is determined theoretically from this field. Measurements are also obtained by varying the gas temperature from 77°K to 700°K. The value of the collision probability for momentum transfer in helium is 18.3 ± 2 percent cm^2/cm^3 per mm Hg from 0 to 0.75 electron volts and increases slowly to a peak value of 19.2 ± 2 percent at 2.2 ev.

IN a recent paper by Phelps, Fundingsland, and Brown,¹ a microwave method was described for determining the probability of collision for momentum transfer by measuring the conductivity of a decaying plasma after the electrons reach thermal equilibrium with the gas. The method has been modified so that a variation in average electron energy from 0.012 to 3 electron volts was obtained. The electron conductivity in the afterglow was studied as a function of experimental parameters and the effects of electron energy, impurities in the gas, ambipolar diffusion, nonuniform electric heating fields, and energy gradients were investigated. The experimental conditions were such that the electron energy distribution function was known. This enabled an expression for the probability of collision for momentum transfer as a function of electron energy to be determined from the experimental data.

ELECTRON CONDUCTIVITY RATIO IN THE AFTERGLOW

Margenau² has given a general theory for the behavior of electrons in a gas under the action of a high-frequency field when only elastic collisions need be considered. From his results the complex electron conductivity σ_c may be written as:

$$\sigma_c = \sigma_r + j\sigma_i = -\frac{4\pi ne^2}{3m\omega} \int_0^\infty \frac{[(\nu_m/\omega) - j] df_0}{1 + (\nu_m/\omega)^2 v^3} dv. \quad (1)$$

Here n is the electron density, e and m are the electronic charge and mass, ω is the radian frequency of the applied field, f_0 is the first term in the spherical harmonic expansion of the normalized electron velocity distribution function for electrons of velocity v . The collision frequency for momentum transfer ν_m is related to the probability of collision for momentum transfer, P_m , by $\nu_m = P_m p_0 v$, where p_0 is the pressure normalized to zero degrees centigrade.

* This work was supported in part by the Signal Corps, the Air Materiel Command, and the U. S. Office of Naval Research.

† Now at Microwave Associates, Boston, Massachusetts.

¹ Phelps, Fundingsland, and Brown, *Phys. Rev.* **84**, 559 (1951).

² H. Margenau, *Phys. Rev.* **69**, 508 (1946).

In a microwave cavity, the quantity which is measured is the electron conductivity averaged with respect to the measuring electric field E_m over the volume of the plasma and is given by the relation

$$\langle \sigma_e \rangle = \langle \sigma_r \rangle + j \langle \sigma_i \rangle = \int_V \sigma_e E_m^2 dV / \int_V E_m^2 dV. \quad (2)$$

Since ν_m is generally a complicated function of velocity, Eq. (1) is difficult to manipulate mathematically. The assumption that $\nu_m^2 \ll \omega^2$ over the velocity range covered by the distribution function f_0 is physically true and simplifies the mathematics. The ratio of the real part of the conductivity to the imaginary part divided by the pressure, designated by ρ , is obtained by Eqs. (1) and (2) yielding

$$\rho = \frac{1}{p_0} \frac{\langle \sigma_r \rangle}{\langle \sigma_i \rangle} = \frac{\int_V n \left[\int_0^\infty (P_m/\omega) v^4 (df_0/dv) dv \right] E_m^2 dV}{\int_V n \left[\int_0^\infty v^3 (df_0/dv) dv \right] E_m^2 dV} \quad (3)$$

for the case $\nu_m^2 \ll \omega^2$. When the energy distribution function is independent of position in the cavity, the quantity ρ is independent of averaging with respect to the electron density and measuring field. Measurements of ρ as a function of energy give information about the velocity dependence of P_m or f_0 . For the more complicated case where f_0 is a function of position in the cavity, the spatial variation of the electron density and the measuring field must be known before any information about P_m or f_0 may be obtained. Equation (3) and the associated conductivity measurements are used in this experiment to obtain the velocity dependence of P_m over as wide a range of velocity as is possible with the present microwave technique. The experimental conditions must be arranged so that the electron energy distribution function is known.

ELECTRON ENERGY DISTRIBUTION FUNCTION

In the afterglow of a pulsed discharge the electrons, whose average energy is high during the discharge, lose their energy through elastic collisions with the gas atoms. Eventually the electrons reach energy equilibrium with the gas atoms and have a Maxwellian distribution with an electron temperature T_e the same as the gas temperature T_g . The electron temperature T_e is defined in terms of the average electron energy by $\langle u \rangle = \frac{3}{2} k T_e$. Above one mm Hg pressure in helium, energy equilibrium is established between electrons and gas atoms within one millisecond after the discharge has ceased. By either heating or cooling the cavity, the electron temperature may be varied over a range of 77°K to 700°K and the distribution function will be Maxwellian. Application of an electric field in a plasma can also increase the average electron

energy. In this case, the energy distribution function, and hence the average energy, will depend upon a balance between the energy gained from the field and the energy lost due to recoil with the gas and the energy transported to the walls by diffusion, conduction, and convection. Energy losses due to inelastic collisions, attachment, and recombination may be neglected. Margenau² has shown the steady state distribution function for electrons in an atomic gas, in the absence of inelastic collisions and diffusion losses, to be Maxwellian under the assumption that $\nu_m^2 \ll \omega^2$. The equivalent electron temperature is given by

$$T_e = T_g + M e^2 E_h^2 / (6 \omega^2 k m^2), \quad (4)$$

where E_h is the applied heating field. However, in a microwave cavity the heating field is a function of position and deviations from Eq. (4) resulting from energy gradients may become important.

The expression for the average energy when the energy is a function of position can be shown to be given by

$$T_e = T_g + a_0 E_h^2 + b_0 \nabla \cdot (n \nabla T_e) / n p_0^2, \quad (5)$$

where

$$a_0 = M e^2 / (6 \omega^2 k m^2) \quad \text{and} \quad b_0 = M / (6 m P_m^2).$$

It is seen that the first two terms, which represent thermal energy and energy gained from the field, are identical with those in Eq. (4). The term containing $\nabla \cdot (n \nabla T_e)$ represents the first-order change in average energy resulting from conduction and convection of energy from regions of high energy to regions of low energy. Equation (5) is derived under the assumption that P_m is constant, which is a good approximation in helium at low energies.

In order to interpret Eq. (3), one must know not only the energy distribution function, but also the electron density distribution. The spatial distribution of the temperature given by Eq. (4) will be used as a first approximation to determine the electron density distribution when the average energy is a function of position. It will be assumed that the dominant electron loss mechanism is ambipolar diffusion.

ELECTRON DENSITY DISTRIBUTION

The correct density distribution can be obtained by solving the ambipolar diffusion equations taking into account the spatial variation of electron energy. The equations³ governing the diffusion of electrons in a space charge field E_s are

$$\Gamma_- = -\nabla(D_- n_-) - \mu_- \mathbf{E}_s n_-, \quad (6)$$

$$\Gamma_+ = -\nabla(D_+ n_+) + \mu_+ \mathbf{E}_s n_+, \quad (7)$$

$$\partial n_\pm / \partial t = \nabla \cdot \Gamma_\pm, \quad (8)$$

where Γ_- and Γ_+ are the electron and positive ion particle currents, n_- and n_+ are the electron and positive ion densities, D_+ and μ_+ are the positive ion diffusion

³ W. Schottky, Physik. Z. 25, 342 (1924).

coefficient and mobility, D_- and μ_- are the electron diffusion coefficient and mobility defined by

$$D_- n_- = \int_0^\infty (v^3/3\nu_m) f_0 4\pi v^2 dv, \quad (9)$$

$$\mu_- n_- = \int_0^\infty (e/3m\nu_m) (\partial f_0/\partial v) 4\pi v^3 dv. \quad (10)$$

For the Maxwellian distribution function whose temperature is given by Eq. (4) D_- and μ_- are functions of position. In solving Eqs. (6), (7), and (8) the usual assumptions of ambipolar diffusion are made, i.e., $\Gamma_+ \approx \Gamma_- = \Gamma$ and $n_+ \approx n_- = n$. Eliminating E_s from Eqs. (6) and (7) one finds

$$\Gamma = [-\mu_+ \nabla(D_- n) - \mu_- \nabla(D_+ n)] / (\mu_+ + \mu_-). \quad (11)$$

Since $\mu_+ \ll \mu_-$ and D_+ and μ_+ are essentially independent of position, Eq. (11) becomes

$$\Gamma = -D_+ [\nabla n + \mu_+ \nabla(D_- n) / D_+ \mu_-]. \quad (12)$$

In order to evaluate Eqs. (9) and (10), the velocity variation of ν_m must be known. The simplest assumption is that $\nu_m = c p_0 v^h$, although any power series in v may be manipulated equally well in the following treatment. The ratio of $\nabla(D_- n) \mu_-$ in Eq. (12) is obtained from Eqs. (9) and (10) by using the above assumption for ν_m :

$$\nabla(D_- n) / \mu_- = (k/e) \nabla(T_e^{(1-h/2)} n) / T_e^{-h/2}. \quad (13)$$

Combining Eqs. (8), (12), and (13) and using the relation $D_+ / \mu_+ = kT_g / e$, one obtains

$$\partial n / \partial t = -D_+ \nabla \cdot [\nabla n + \nabla(T_e^{(1-h/2)} n) / T_g T_e^{-h/2}]. \quad (14)$$

It is assumed that the variation of density with time has the form

$$n = n_0 \exp(-\gamma t), \quad (15)$$

and, hence, Eq. (14) becomes

$$(1 + T_e/T_g) \nabla^2 n + (2 - h/2) \nabla n \cdot \nabla(T_e/T_g) + n [(1 - h/2) \nabla^2(T_e/T_g) + \gamma/D_+] = 0. \quad (16)$$

The problem consists of solving Eq. (16) for its characteristic functions corresponding to the proper boundary condition, proper spatial variation of T_e , and a given value of h . In general, the characteristic function corresponding to the lowest characteristic value is the important physical solution. Equation (16) is solved for two different cavities. One is a rectangular parallelepiped in which the plasma fills the entire cavity; the other is also a cavity of the same shape but with the plasma contained in a cubical bottle concentric with the cavity. The applied electric field has a spatial configuration corresponding to the fundamental mode of the cavity and is a function of only two coordinates. The boundary conditions for the cavity are that the electron density vanish along the walls of dimension A , B , and C and for the bottle

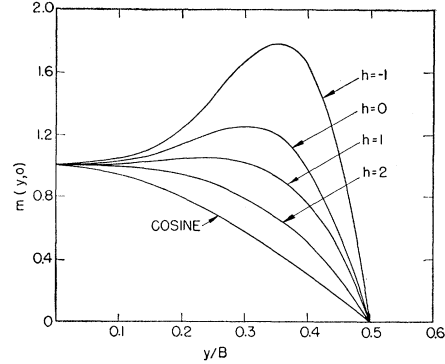


Fig. 1. Electron density as a function of position for various values of h and $T_{e0}/T_g = 4$.

that the density vanish along the walls of dimension d . The dimensions of this particular cavity are $A = 7.16$ cm, $B = 7.88$ cm, and $C = 6.48$ cm. The dimensions of the cavity containing the bottle are $A = 6.90$ cm, $B = 7.51$ cm, $C = 6.28$ cm, and the dimension of the bottle is $d = 2.82$ cm.

Since the heating field is a function of two directions, y and z , the electron density may be written as $n = n_0 m(y, z) \cos(\pi x/A)$. Equation (16) may be separated into a two-dimensional second-order differential equation which is solved numerically by relaxation techniques. The results for the cavity in which the plasma fills the entire volume are best depicted by plotting $m(y, z)$ as a function of y/B for $z = 0$ and are shown in Fig. 1. The curves give $m(y, 0)$ for various values of h for T_{e0} , the electron temperature at the center of the cavity, equal to $4T_g$. The curves are compared with a cosine distribution which is the solution of Eq. (16) when the temperature distribution is independent of position. For larger ratios of T_{e0}/T_g , the deviation from a cosine distribution increases.

The shape of the curves in Fig. 1 for the various values of h is readily explainable. The off-center maximum is caused by the lower temperature near the walls, the electron pressure decreasing monotonously toward the walls. This effect is enhanced for $h < 2$ as then the diffusion coefficient increases with temperature, resulting in a flatter electron pressure distribution near the center with steep gradients near the walls. In Fig. 2 curves of $m(y, 0)$ as a function of y/B are shown by the solid curves when $h = 1$, i.e., P_m constant, for a range of T_{e0}/T_g from 4 to 11. The curves illustrate the increase in the density distribution peaks near the walls as the electron temperature T_{e0} increases. From the results shown, it is obvious that in any calculations involving the density averaged over the volume of the plasma it is necessary to use the proper density distribution.

A similar calculation was performed for the cavity containing a cubical bottle of dimension d . The results are shown by the dotted curves in Fig. 2 for $h = 1$ and

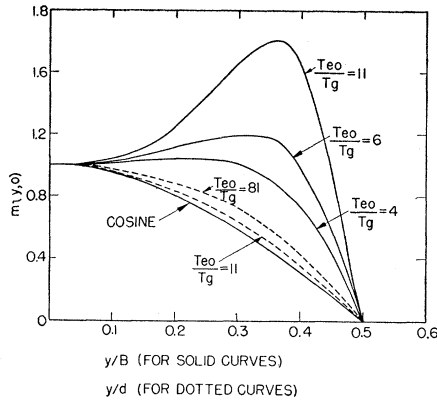


FIG. 2. Electron density as a function of position for various values of T_{e0}/T_g and $h=1$.

$T_{e0}/T_g=11$ and 81. Since the nonuniformity of the heating field is small over the volume of the bottle, the deviation of the curves from a cosine is negligible. Hence, over this region of electron temperature, a cosine distribution is sufficiently accurate for representing the density distribution provided that ambipolar diffusion is the dominant loss mechanism.

ELECTRON CONDUCTIVITY RATIO FOR CONSTANT COLLISION PROBABILITY

When the energy distribution function is Maxwellian, the conductivity ratio given by Eq. (3) becomes

$$\rho = \rho_0 \int_V n(T_e/T_g)^{3/2} E_m^2 dV / \int_V n E_m^2 dV, \quad (17)$$

where $\rho_0 = 1.505(P_m/\omega)(2kT_g/m)^{3/2}$ for the case when the collision probability is constant. This is approximately valid for helium. The solution of Eq. (17) is considered when a heating field is present. The electron density distribution is predicted by the theory of ambipolar diffusion in a nonuniform field and the electron temperature is given by Eq. (5). Thus the effects of a nonuniform heating field and the associated energy gradients on the electron density and temperature distributions are included to a first-order approximation. For the cavity in which the plasma fills the entire volume, the solution of Eq. (17) for T_{e0}/T_g greater than 10 is given approximately by

$$\rho = \rho_0 f(T_{e0}/T_g) (1 + 3/\rho_0^2). \quad (18)$$

The function $f(T_{e0}/T_g)$ is obtained from a numerical integration of Eq. (17). Below $T_{e0}/T_g=10$, the correction factor $3/\rho_0^2$, decreases becoming zero at $T_{e0}/T_g=1$. We can see from Eq. (18) that at pressures below 10 mm Hg, the influence of energy gradients becomes important and the value of ρ increases.

A similar calculation is performed for the bottle enclosed in a cavity, yielding the following expression valid for T_{e0}/T_g greater than 10:

$$\rho = \rho_0 0.93 [(T_{e0}/T_g) - 1]^{3/2} [1 + 0.03/\rho_0^2]. \quad (19)$$

At a pressure of 1 mm Hg or below, the perturbation term becomes important. It should be remembered that the condition of $\nu_m^2 \ll \omega^2$ is imposed throughout the discussion. In order to insure that $\nu_m^2 \leq 0.04\omega^2$, at a frequency of 3000 megacycles one must have

$$p_0 \leq 350/T_e^{1/2}. \quad (20)$$

Therefore, 2000°K is approximately the maximum temperature that can be maintained in the cavity alone before gradients have an important influence and still satisfy the condition of Eq. (20). In the bottle 25 000°K is approximately the maximum temperature. From the above discussion, it follows that the conductivity measurements above thermal energies should be made in a bottle so that a wide range of electron energy can be obtained without introducing complicated correction factors into the theory. For this case, when ambipolar diffusion is the dominant loss mechanism, the density distribution is well approximated by a cosine distribution and the electron temperature is determined by Eq. (4).

EXPERIMENTAL PROCEDURE

The technique used for measuring the electron conductivity ratio ρ is described in a paper by Gould and Brown.⁴ The presence of a plasma introduces a change in the conductance and susceptance of the cavity. This change can be determined by measuring the ratio of the microwave power transmitted through the cavity to the power incident as a function of signal frequency in the vicinity of cavity resonance. The microwave cavity used in the experiment is a rectangular parallelepiped and is designed to resonate in its three fundamental modes at wavelengths of 9.5, 10.0, and 10.5 cm. The 9.5-cm mode is used to produce a pulsed discharge in helium of variable pulse length. The 10.0-cm mode is used to increase the average electron energy in the afterglow, and the 10.5-cm mode is used to measure the characteristics of the plasma. The apparatus and procedure associated with each mode will be discussed separately and will be referred to as the breakdown mode, heating mode, and measuring mode. The general block diagram of the experimental microwave equipment is shown in Fig. 3. $\frac{7}{8}$ -in. coaxial transmission line is used throughout.

In the breakdown mode, a tunable pulsed magnetron (QK61), supplying 100-watts peak power, is used to produce a pulsed discharge in the cavity. This magnetron is pulsed for a duration varying between 0.1 to 5 milliseconds and at a repetition rate varying from 20 to 120 cps. A well regulated pulsed voltage supply, used to modulate the magnetron output, is necessary in order to stabilize the discharge so that accurate measurements in the afterglow can be performed.

In the measuring mode, a continuous-wave tunable magnetron (QK59) is used for measuring the conduc-

⁴L. Gould and S. C. Brown, J. Appl. Phys. 24, 1053 (1953).

tivity ratio during the afterglow. The microwave power, incident on the cavity, is adjusted by the proper attenuation to a few microwatts so that the value of the measuring electric field is less than 0.1 volt/cm. The perturbation of the plasma characteristics from a field of this value is negligible. The ratio of the transmitted power to the incident power is measured by the power measuring section which uses transient receivers.⁵ These receivers are operative for a period of 20 to 100 microseconds and can be delayed in time with respect to the breakdown pulse so that any time in the afterglow can be measured. At a particular time in the afterglow, the signal frequency is adjusted to the resonant frequency of the cavity and plasma, and the apparent ratio of the incident to transmitted power is adjusted to unity by varying the gain of the receivers. A plot of the change in this ratio as a function of the square of the signal frequency change from resonance is linear. The frequency change is measured directly by the frequency measuring section. Similar measurements are obtained with no plasma in the cavity. The difference in the slopes of the linear plots with and without a plasma present (plasma conductance) divided by the difference in the resonant frequency for both cases (plasma susceptance) yields the ratio of the real to the imaginary part of the conductivity, σ_r/σ_i . The accuracy of the conductivity measurements by this null technique is ± 2 percent.

In the heating mode, a continuous wave tunable magnetron (QK60) is used for producing the electric field in the cavity which increases the average electron energy. Measurements of the unloaded Q , obtained from standing wave ratio measurements as a function of signal frequency, and the power incident on the cavity, determine the electric field in the cavity within an accuracy of ± 3 percent. In the afterglow of a discharge the electric field, for a constant incident power, will be a function of the electron density. The electric field will have a maximum value at that time in the afterglow when the signal frequency corresponds to the resonant frequency of the cavity and plasma.

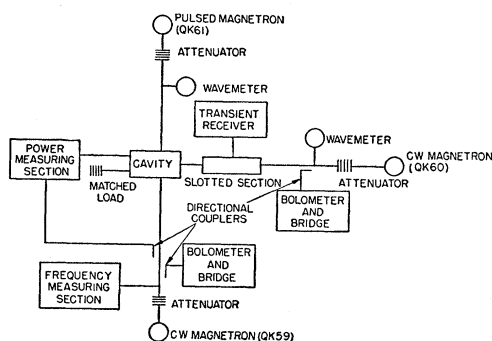


FIG. 3. General block diagram of experimental equipment.

⁵ Rose, Kerr, Biondi, Everhart, and Brown, Technical Report No. 140, Research Laboratory of Electronics, Massachusetts Institute of Technology (unpublished).

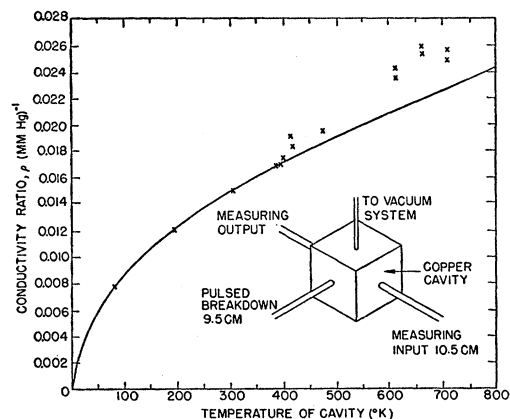


FIG. 4. Conductivity ratio as a function of cavity temperature. The x 's are the experimental points and the solid line the theoretical curve for $P_m = 18.3$.

The electric field should remain constant for a sufficiently long time so that the electrons can reach equilibrium with the electric field. If the unloaded Q of the cavity is low, the change in Q due to the presence of plasma will be small, thus minimizing the variation of the electric field with electron density. An output loop connected to a matched load is adjusted so that it only couples out power from the heating mode. By changing the coupling between the cavity and the matched load, an additional loss is reflected back into the cavity and the unloaded Q for this mode, measured at the input terminals of the cavity, decreases. A decrease in Q_u from 5000 to 200 is easily obtained by this method. For the applied fields used in this experiment, the time necessary for equilibrium is of the order of tenths of milliseconds. Unloaded Q 's of the order of several hundred allow the electric field to remain constant for the order of a millisecond thus insuring equilibrium with the field. It is during this interval of time that the electron conductivity ratio is measured.

For the vacuum system, a standard forepump and a three stage oil diffusion pump are used in conjunction with metal valves⁶ wherever necessary. The helium pressure is measured by a McCleod gauge calibrated to an accuracy of ± 1 percent over a range of 0.10 to 20 mm Hg. The method for introducing the helium is as follows: A "fritted" glass filter, one end of which has a break-off seal, is connected to the main vacuum system by a metal valve. The glass filter may be placed in a liquid helium Dewar flask. A liter Pyrex bottle, connected to the cavity side of the system by another valve, serves as a reservoir for the helium. After the system is baked, a vacuum of about 10^{-7} mm Hg is obtained when the system is isolated from the pumps. At this point liquid helium is poured into the Dewar flask. When the "fritted" glass filter is completely immersed in the liquid helium, the break-off seal is broken and helium is evaporated into the system.

⁶ S. C. Brown and J. E. Coyle, Rev. Sci. Instr. 23, 570 (1952).

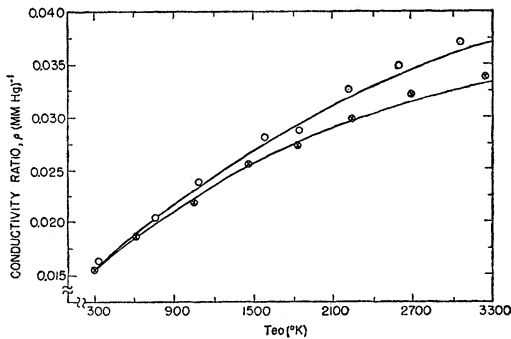


FIG. 5. Conductivity ratio as a function of the electron temperature at the center of the cavity. Experimental points for $p_0=5$ mm Hg and x 's for $p_0=10$ mm Hg. The solid lines are calculated theoretically.

If impurities are present, experimentally measured values of ρ are not independent of pressure or time as indicated by Eq. (3). Constancy of ρ as a function of these variables was taken as a measure of gas purity, and the helium produced from liquid helium as just described met these conditions.

RESULTS

Measurements of ρ as a function of gas temperature and pressure were obtained in a copper cavity. Provisions were made for cooling the cavity to dry ice (195°K) and liquid air (77°K) temperatures and for heating the cavity from room temperature to 400°C. The results are shown in Fig. 4. Included in the figure is a sketch of the cavity showing the relative positions of the coupling lines for the measuring mode and the pulsed breakdown mode. The crosses represent the experimental points and the solid line represents the theoretical curve for ρ when P_m is constant and equal to 18.3 cm²/cm³ per mm Hg. According to Eq. (17), for the case of P_m constant, ρ is given by

$$\rho = 1.505(P_m/\omega)(2kT_e/m)^{3/2}. \quad (21)$$

It is seen that the experimental points agree with the above equation over the range of 77°K to 400°K. Above 400°K, the values of ρ obtained are higher than the theoretical curve. It is believed that impurities liberated from the walls of the cavity at the higher temperatures produced the higher values of ρ . At a given temperature, the high values of ρ could be lowered by outgassing the cavity for several days at a temperature of 430°C.

Measurements of ρ as a function of the heating electric field were obtained in the copper cavity. The electric field was measured according to the usual microwave techniques.⁵ Transient operation was used to measure the Q of the heating mode simultaneously with the electron conductivity measurements. The results are shown in Fig. 5. The experimental data are represented by the crosses and points. The dotted curves are theoretical results for ρ corresponding to

Eq. (18) in which the effects of energy gradients are included and P_m is 18.3 cm²/cm³ per mm Hg and constant. It is seen that the predicted increase in ρ due to the importance of energy gradients is evident from the data at 5 mm Hg. At $T_{e0}=3300^\circ\text{K}$ the difference between the theoretical curves for $p_0=5$ mm and 10 mm Hg is 12 percent. The experimental data show that the density distribution predicted from the theory of ambipolar diffusion in nonuniform fields is the proper one. In general, interpretation of measurements in the cavity would be rather difficult for gases in which P_m is not known, since a knowledge of P_m is necessary to calculate the proper density distribution for the evaluation of ρ .

Measurements of ρ as a function of the heating electric field were also obtained for the case of the bottle enclosed in the cavity. The averaged experimental results for ρ as a function of the electron temperature are shown in Fig. 6. The scatter in data is ± 2 percent. The relation between the electron temperature and the electric field is given by Eq. (4) which, for helium, is $T_{e0}=(T_g+72.5E_0h^2)$, where the field is in volts/cm. Included in Fig. 6 is a sketch of the cavity and bottle showing the relative positions of the coupling lines for the measuring, heating, and breakdown modes.

The relation between ρ and P_m depends upon the spatial distribution of the electron density and the electric field. The electric field configuration is assumed to be that of the fundamental mode. The electron density distribution is assumed to be cosinusoidal. If a power series in velocity is assumed for P_m , the collision probability, is of the form

$$P_m = b_1 + b_2v + b_3v^2. \quad (22)$$

Equation (3) becomes

$$\rho = \sum_{s=1}^3 A_s I_s, \quad (23)$$

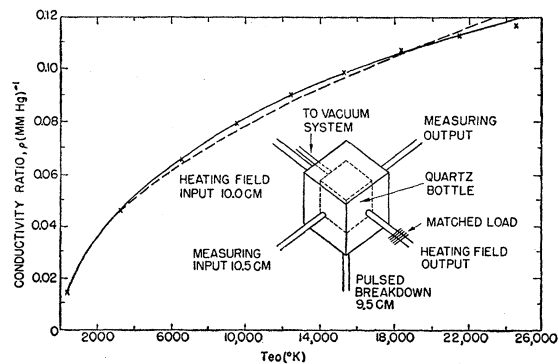


FIG. 6. Conductivity ratio as a function of the electron temperature at the center of the quartz bottle. The solid line represents the experimental curve, the dotted line the theoretical curve, $P_m=18.3$, and the x 's are calculated from the power series approximation.

where

$$A_s = (2kT_g/m)^{s/2} b_s [(3+s)/2]! \omega (3/2)!,$$

$$I_s = \left[\int_V n (T_e/T_g)^{s/2} E_m^2 dV \right] / \int_V n E_m^2 dV$$

$$= 1.065 \int_0^{\pi/2} \int_0^{\pi/2} (1 + a \cos^2 0.393u \cos^2 0.449w)^{s/2} \\ \times \cos w \cos u \cos^3 0.393dw du,$$

and $a = 0.241 E_{0h}^2$ when $T_g = 300^\circ\text{K}$.

The expression I_s can be calculated analytically when s is an even number and must be calculated numerically when s is an odd number. I_s is only a function of the electric field, E_{0h} . When P_m is equal to 18.3 and constant (s equal to one) the plot of ρ as a function of T_{e0} is shown in Fig. 6 as the dotted curve. The experimental and the theoretical curves agree up to a temperature of 4000°K . At low electron energies, both the thermal and the heating field measurements yield the same value for P_m . This indicates that the higher values of ρ obtained in the thermal measurements above 400°K are not the true values but are probably due to impurities. For a more accurate determination of the velocity dependence of P_m , the experimental curve for ρ can be expressed in terms of a series in I_s . The coefficients A_s are determined from the experimental curve in Fig. 6. The values of b_s can be obtained from the values of A_s , according to Eq. (23), giving the following expression for P_m :

$$(P_m = 18.1 + 2.91 \times 10^{-8}v - 2.1 \times 10^{-16}v^2), \quad (24)$$

where v is in cm per second.

A plot of the momentum transfer collision probability as a function of electron velocity in square root of

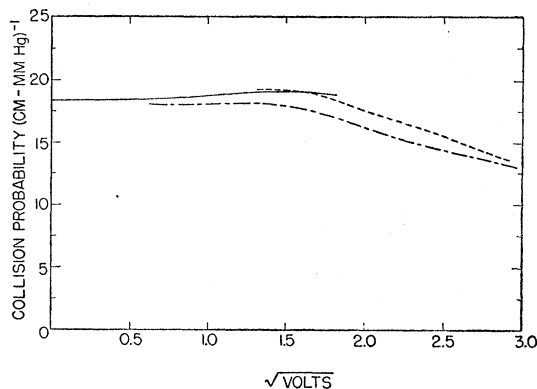


FIG. 7. Collision probability of electrons in helium as a function of electron velocity. Solid line is the momentum transfer collision probability as determined by the microwave method. Short-dash line represents the collision as measured by Normand. Long-and-short-dash line gives the momentum transfer collision probability calculated from the measurements of Normand, Ramsauer and Kollath.

volts is shown as a solid curve, in Fig. 7. This plot is compared with the total collision probability data of Normand⁷ using the dc method. Below a velocity of 1.5 volts^{1/2}, Normand's data have an oscillatory behavior. Since the microwave method cannot distinguish such a behavior, the curve shown in Fig. 7 is an average of Normand's data. In addition, the momentum transfer collision probability for the dc method is derived by using Normand's data and the angular distribution data of Ramsauer and Kollath.⁸ It is seen that there is good agreement between the microwave and the dc method.

The authors wish to acknowledge the technical assistance of Mr. J. J. McCarthy.

⁷ C. E. Normand, Phys. Rev. **35**, 1217 (1930).

⁸ C. Ramsauer and R. Kollath, Ann. Physik **12**, 529 (1932).